NRC Research Press

ARTICLE

Dynamic response of vertically loaded helical and driven steel piles

Mohamed Elkasabgy and M. Hesham El Naggar

Abstract: The dynamic performance of helical piles is of significant interest because such piles can offer an efficient alternative to conventional piling systems in many applications where the foundation is subjected to dynamic loads. This paper presents the results of full-scale dynamic vertical load tests on a 9.0 m double-helix, large-capacity helical pile and a driven steel pile of the same length and shaft geometry. Comparing the results is considered necessary to evaluate, qualitatively and quantitatively, the dynamic performance characteristics of large-capacity helical piles. The test piles were closed-ended steel shafts with an outer diameter of 324 mm. The piles were subjected to harmonic (quadratic) loading of different force intensities acting within a frequency range that covered the resonant frequencies of the tested pile–soil–cap systems. The dynamic and static properties of the subsurface soil adjacent to the test piles were determined using the seismic cone penetration technique and the conventional soil boring and testing methods. In addition, field observations are compared with calculated responses using the program DYNA 6 to better understand the pile–soil interaction for the case of helical piles. The effects of soil nonlinearity and pile–soil separation were accounted for in the analysis by employing a weak boundary zone around the piles in the analytical model. The experimental results show that the dynamic behaviour of helical piles is essentially the same as that of driven steel piles with the same geometric properties (without the helix plates). In addition, it was demonstrated that the program DYNA 6 can accurately simulate the behaviour of both helical and driven piles.

Key words: vertical vibrations, machine foundations, nonlinear vibration, helical piles, driven piles, full-scale dynamic testing.

Résumé : La performance dynamique de pieux hélicoïdaux est d'intérêt significatif puisqu'ils peuvent offrir une alternative efficace aux systèmes de pieux conventionnels dans plusieurs applications où la fondation est soumise à des sollicitations dynamiques. Cet article présente les résultats d'essais de chargement dynamique vertical à l'échelle réelle sur un pieu hélicoïdal à double hélice, de grande capacité, de 9,0 m, et d'un pieu foncé en acier de même longueur et de même géométrie de l'arbre. La comparaison des résultats s'avère nécessaire pour évaluer, qualitativement et quantitativement, les caractéristiques de la performance dynamique de pieux hélicoïdaux de grande capacité. Les pieux d'essai étaient faits d'un arbre d'acier à embouts fermés avec un diamètre externe de 324 mm. Les pieux ont été soumis à des sollicitations harmoniques (quadratiques) de différentes intensités de force agissant à l'intérieur d'une gamme de fréquences qui couvre les fréquences résonnantes des systèmes pieu-sol-cap testés. Les propriétés dynamiques et statiques du sol de fondation adjacent aux pieux d'essai ont été déterminées à l'aide de la technique sismique de pénétration du cône ainsi que par des méthodes conventionnelles de forage et d'essais de sol. De plus, les observations de terrain sont comparées aux résultats calculés avec le programme DYNA 6 afin de mieux comprendre l'interaction sol-pieu dans le cas de pieux hélicoïdaux. Les effets de la non linéarité du sol et de la séparation pieu-sol ont été considérés dans l'analyse en utilisant une zone frontière faible autour des pieux dans le modèle analytique. Les résultats expérimentaux démontrent que le comportement dynamique de pieux hélicoïdaux est essentiellement le même que celui de pieux d'acier foncés avec les mêmes propriétés géométriques (sans les plaques hélicoïdales). Il a aussi été démontré que le programme DYNA 6 peut simuler de façon juste le comportement de pieux autant hélicoïdaux que foncés. [Traduit par la Rédaction]

Mots-clés : vibrations verticales, fondations machinées, vibration non linéaire, pieux hélicoïdaux, pieux foncés, essai dynamique à l'échelle réelle.

Introduction

Helical piles are gaining popularity in several engineering applications because of their ease of installation — with low levels of noise and vibration — and superior performance in certain soil profiles compared to the conventional piling systems such as driven steel piles. Furthermore, helical piles allow immediate loading upon installation and can be installed through ground water without casings, unaffected by caving soils (Bobbitt and Clemence 1987). Helical piles are mostly designed to sustain static loading (Adams and Klym 1972; Carville and Walton 1995; Zhang 1999; El Naggar and Abdelghany 2007*a*, 2007*b*; Sakr 2009). Such applications include transmission towers, pipelines, residential and industrial buildings, and supporting retaining structures.

Piles are commonly employed to support foundations subjected to dynamic loads, such as those produced in power generation and petrochemical plants, oil refineries, offshore structures, and wind turbines. The dynamic response of these foundations depends on the dynamic impedances (i.e., stiffness and damping) of the supporting piles, which in turn is a function of the pile–soil interaction. Numerous theoretical studies have been conducted to evaluate the dynamic response and impedance functions of piles, including lumped mass models (Penzien 1970; Kuhlemeyer 1981), Winkler models (El Naggar et al. 2005), finite element methods (Kuhlemeyer 1979; Manna and Baidya 2009), cone models (e.g., Wolf et al. 1992), and the continuum approach (e.g., Baranov 1967). Novak and his co-workers (Novak 1974, 1977; Nogami and Novak

Received 22 March 2011. Accepted 6 November 2012.

M. Elkasabgy. AMEC E&I, 140 Quarry Park Blvd. S.E., Calgary, AB T2C 3G3, Canada.
M.H. El Naggar. Geotechnical Research Centre, Faculty of Engineering, The University of Western Ontario, London, ON N6A 5B9, Canada.
Corresponding author: M. Hesham El Naggar (e-mail: helnaggar@eng.uwo.ca).

1976; Novak and El Sharnouby 1983) simplified the continuum approach by introducing the plane strain theory for the calculation of the impedance functions of piles. This simplified approach accounts for pile-soil interaction and energy dissipation through elastic wave propagation within the soil continuum. Novak and Aboul-Ella (1978*a*, 1978*b*) extended the theoretical formulations for piles embedded in layered soil media. Novak and Sheta (1980) introduced the concept of a weak soil boundary zone around the pile to account for soil nonlinearity and pile–soil separation. El Naggar and Novak (1992, 1994) analyzed the pile axial response to harmonic loading while allowing for nonlinear soil behaviour, energy dissipation through geometrical damping, hysteretic damping, and loading rate dependency of the soil resistance.

The dynamic behaviour of piles was also investigated through experimental studies. For example, Blaney et al. (1987) conducted a large-amplitude vertical vibration test of a full-scale group of nine driven piles and two single piles. El Marsafawi et al. (1992) carried out field experiments on two groups of steel and concrete piles to investigate the ability of linear elastic theories to predict the response characteristics of piles. Forced vibration tests of a full-scale, cast-in-situ, expanded-base concrete pile supporting a structural mass were reported by Sy and Siu (1992) and the experimental responses were compared with the theoretical results of the plane strain approximate solutions. In addition, small-scale field experiments were conducted to assess the dynamic characteristics of piles. Novak and Grigg (1976) and Sheta and Novak (1982) executed small-scale field dynamic tests on groups of four piles installed in silty sand soil, while El Sharnouby and Novak (1984) tested a large group of 102 closely spaced small piles vibrating with small amplitudes to verify the available linear theories.

For foundations supported on helical piles, the evaluation of stiffness and damping involves consideration of the interactive forces between the pile and the soil along the pile shaft and at the helices. Thus, the analysis requires proper understanding of the load-transfer mechanism during the dynamic loading. The dynamic behaviour of large-capacity helical piles with one or more helices has never been investigated thoroughly (Elkasabgy et al. 2010). Thus, there is a need to develop a reliable method of analysis that can be used to calculate the stiffness and damping constants of large-capacity helical piles.

Objectives and scope of work

The main objectives of this study are to investigate the performance characteristics of single large-capacity helical and driven piles under vertical harmonic vibrations to identify a suitable methodology to evaluate the impedances of helical piles. Both full-scale field testing and theoretical analysis are described. The response curves and load-transfer mechanisms of the piles were established from the experimental measurements under several excitation intensities and compared with those calculated using the computer program DYNA 6. Two approaches were adopted in the analysis based on the Novak's continuum theory: linear and nonlinear.

Subsurface conditions

The test site is located in Ponoka, Alberta, Canada. The surficial deposits in the area of the test site consist of Pleistocene Stagnation Moraine glacial till depositions. Both in situ and laboratory tests were performed to characterize the dynamic and static properties of the site soils. Laboratory tests were conducted on disturbed and undisturbed samples collected from one borehole at an interval of 1.5 m. Standard penetration tests (SPT) were performed in the borehole to determine the *N*-value at different depths. The dynamic in situ test consisted of three seismic cone penetration tests (SCPT) carried out to a depth of 15 m. The SCPT results were used to determine the soil layering and the distribution of the small-strain shear and compression wave velocities, V_s and V_p, respectively, with depth, as shown in Figs. 1–3. The subsurface investigation indicated that the site at the location of the test piles consists of a sandy silt crust 1.5 m thick. The crust is underlain by a 3.0 m thick layer of stiff brownish clay to silty clay and clayey silt interbedded with seams of silt, followed by interbedded layers of very stiff grey silty clay, clayey silt, and clay. This is underlain by a small layer of dense to very dense silty sand underlain by a layer 7.2 m thick of very stiff to hard grey clay till, with low to medium compressibility, overlaying interbedded layers of sandy silt, silt, clayey silt, and silty clay. The ground water level was determined to be at about 2.0 m below the ground surface. The values of soil shear wave velocity, V_s, were obtained from the measurements of the SCPT and from the established empirical correlations in terms of the measured cone tip resistance, q_t, and effective overburden pressure, σ'_{vo}, i.e., Mayne and Rix (1995) cohesive soils

Fig. 1. Plan view of piles, seismic cone penetration tests, and borehole.

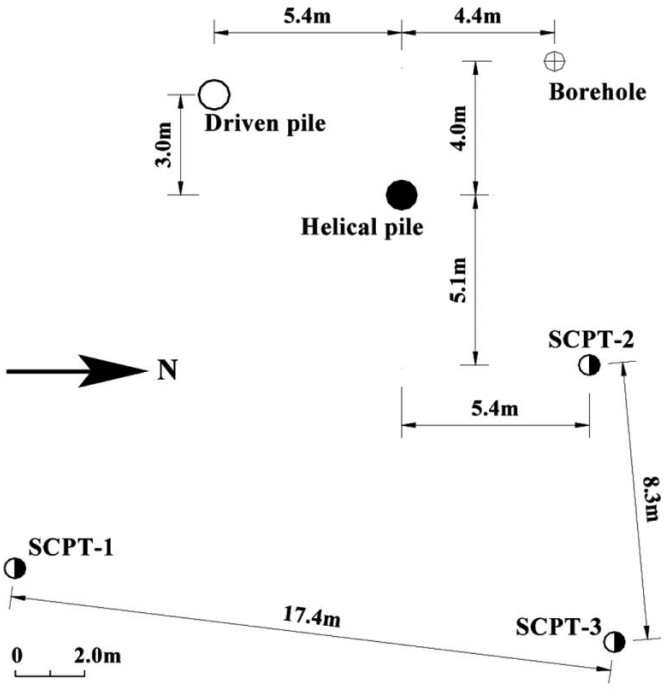

$$V_s = 1.75(q_t)^{0.627} \quad (1)$$

where q_t is in kPa, and Baldi et al. (1989) cohesionless soils

$$V_s = 277(q_t)^{0.13}\left(\sigma'_{vo}\right)^{0.27} \quad (2)$$

where q_t and σ'_{vo} are in MPa.

Due to the small varying thickness of the silty sand layer and the fact it was sandwiched between two very stiff clayey soils, which might have affected the accuracy of its measured V_s, it was deemed reasonable to consider an average value of its shear wave velocity (V_s = 200 m/s). On the other hand, the values of Poisson's ratio, ν, were obtained from the V_s and V_p measurements, and found to vary between 0.35 and 0.49. Such high Poisson's ratios were considered to have insignificant influence on the dynamic response of the soil–pile system based on Dobry et al. (1982). Finally, the shear modulus, G_o, of the soil was determined using the elastic theory, i.e., $G_o = \rho V_s^2$, where ρ is the mass density of soil. Figure 4 presents the variation of the small-strain dynamic prop-

Fig. 2. Distribution of cone tip resistance, sleeve friction, friction ratio, and pore pressure at SCPT-2 and distribution of SPT *N*-values at borehole. (1 bar = 100 kPa.)

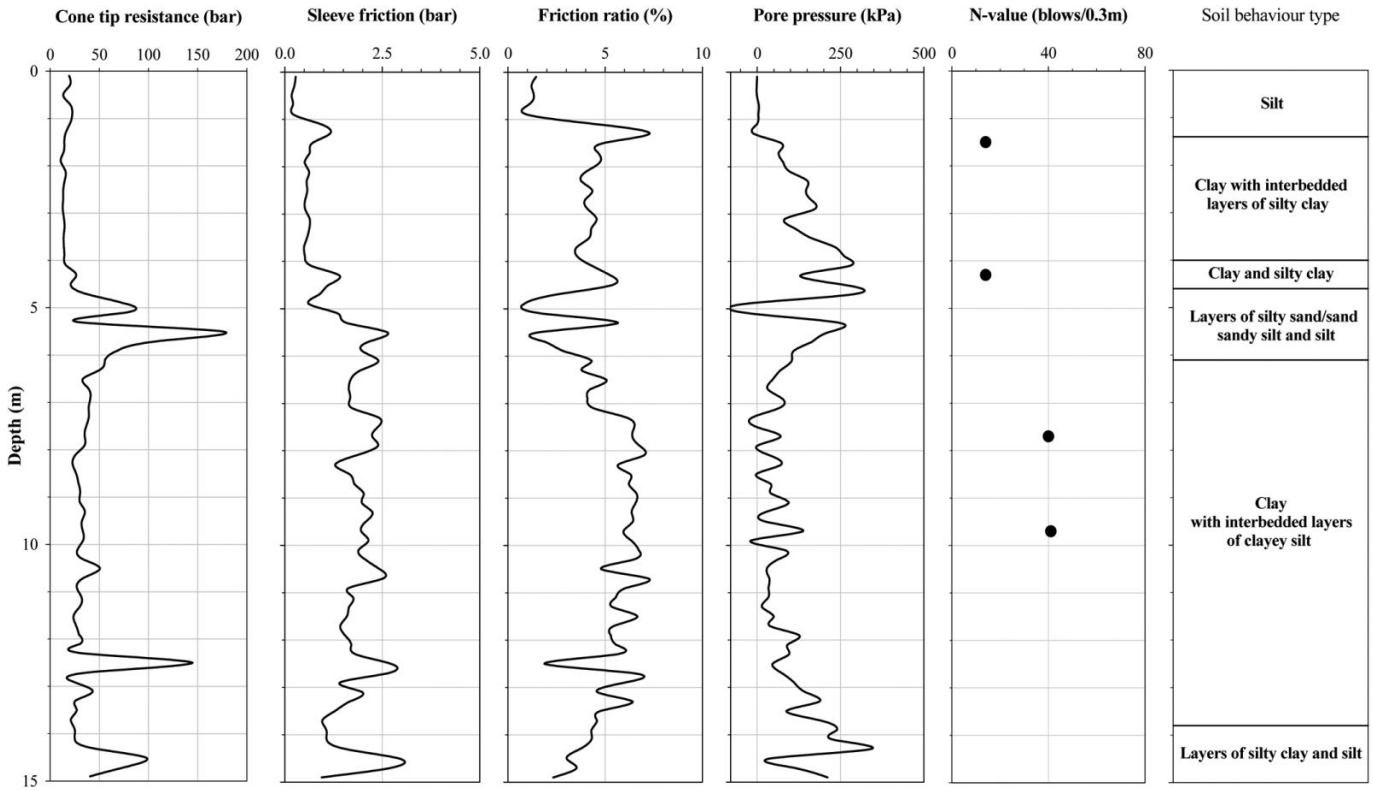

erties, Poisson's ratio, bulk unit weight (γ), moisture content (W_c), and specific gravity (G_s), of the site soils.

Experimental setup

Test piles

The helical pile was 9.0 m long and was composed of a steel pipe shaft with a diameter of 324.0 mm and wall thickness of 9.0 mm. It had two helices; each was 0.61 m in diameter with an interhelix spacing of 0.91 m (1.5 times helix diameter). The leading edge of the helical plate was rounded back and sharpened to facilitate the installation of the pile with minimal soil disturbance, while the pile toe was cut at 45° to aid in targeting the pile during installation. The pile was closed-ended with a flush closure steel plate. The pile was installed by applying a clockwise turning moment (torque) to the pile shaft, by a hydraulic torque head, while sustaining a constant rate of penetration of one helix plate pitch (152.4 mm) per revolution. The pile protruded 0.6 m above the ground surface (i.e., unsupported length). The driven pile was closed-ended and had material properties, pile length, shaft diameter, and wall thickness similar to the helical pile shaft, but had no helices. The pile was installed using a mechanical drop hammer weighing 5000 kg. Table 1 provides all required geometrical and material properties of the test piles.

Test body

To ensure that the resonant frequencies were well defined and within the frequency range of the excitation machine, and to simulate the effects of a superstructure on the response of the pile–soil system, a steel test body was added on top of the pile cap. The pile cap was a machined rectangular steel plate, weighing approximately 88 kg. The head of the pile was machined after its installation to keep a clean levelled edge to facilitate welding of the cap perpendicular to the centreline of the pile. The steel test body plates were then stacked on top of the pile cap. The test body comprised 59 machined circular steel plates; each with a 79 kg mass. The steel plates had machined contact surfaces to prevent slippage between the plates and they were rigidly fastened together so that the whole setup acted as a rigid body. The schematic diagram of the experimental setup is shown in Fig. 5.

Excitation mechanism

The vertical excitation force was produced by a Lazan mechanical oscillator (Model MO2460) mounted over the test body mass. The excitation force was quadratic and characterized by harmonic forces proportional to the square of the driving frequency. The oscillator comprised two counteracting shafts; each carried a set of eccentric masses to generate the harmonic excitation. The magnitude of the excitation force was varied by altering the degree of eccentricity of the rotating unbalanced masses via an external knob at the end of one shaft assembly. The oscillator had a mass of 51.5 kg and was driven by a 7.5 HP, 220 V, three-phase motor capable of generating a sinusoidal force of 23.5 kN peak-to-peak. The speed of the motor was controlled by a variable frequency AC speed drive, yielding stable operating speeds between 3 and 60 Hz. A well-balanced, flexible drive shaft was utilized to connect the oscillator to the motor through its end couplings.

The oscillator was placed on the top of its base plate, which was welded to the upper steel plate of the test body mass. Four holding rods were used to connect the holding channel frame to the oscillator base plate to keep the oscillator stable under vibration. To produce vertical load, the oscillator was placed horizontally on its base plate. Table 2 gives the properties of the test body, oscillator, and pile cap.

Instrumentation

The vibration measuring equipment consisted of two uniaxial piezoelectric accelerometers, one triaxial accelerometer, and a frequency measurement unit (tachometer) to monitor excitation

Fig. 3. Measured and estimated dynamic properties from the seismic cone penetration tests: (*a*) SCPT-1; (*b*) SCPT-2; (*c*) SCPT-3.

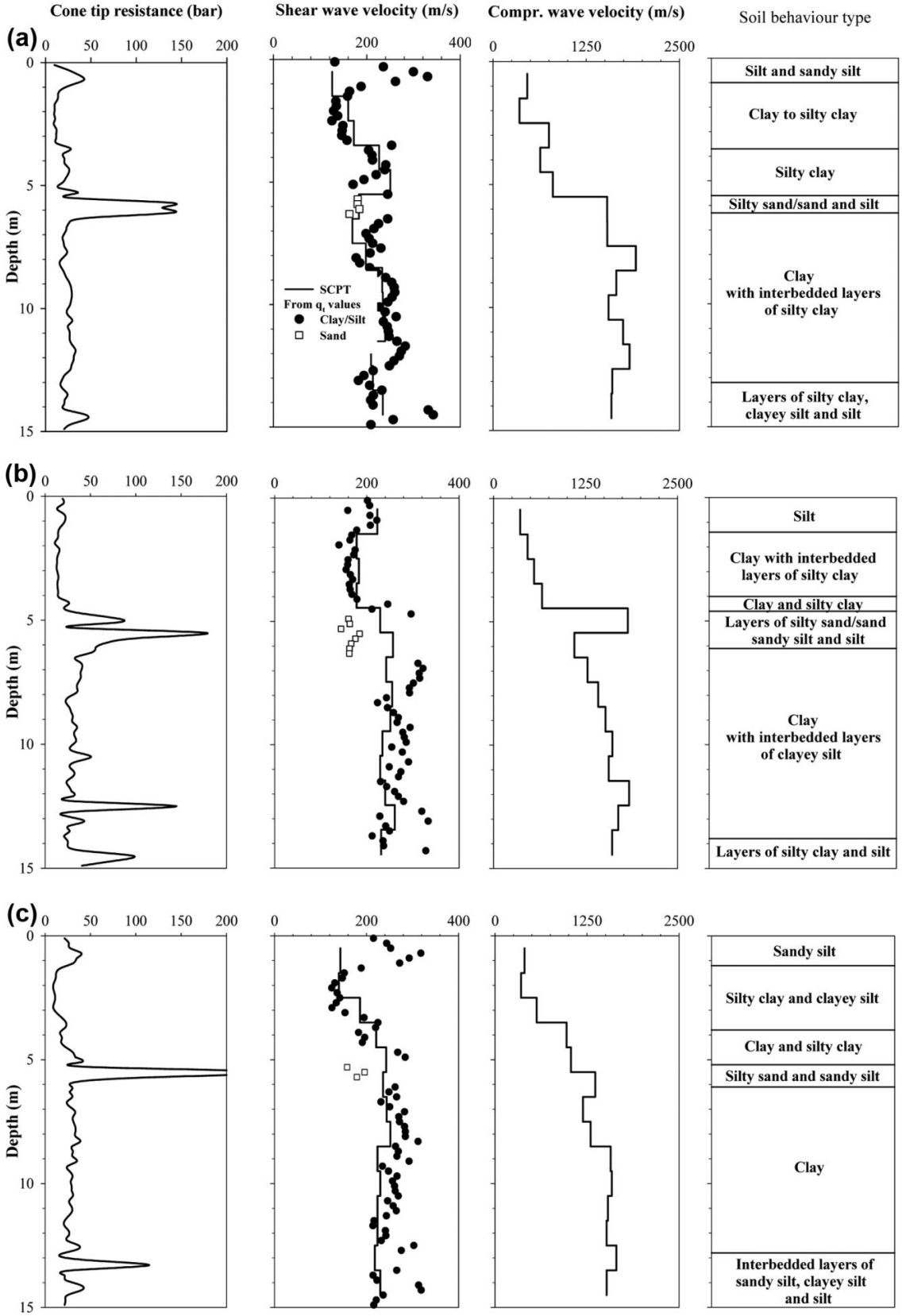

Fig. 4. Measured dynamic and index properties with depth.

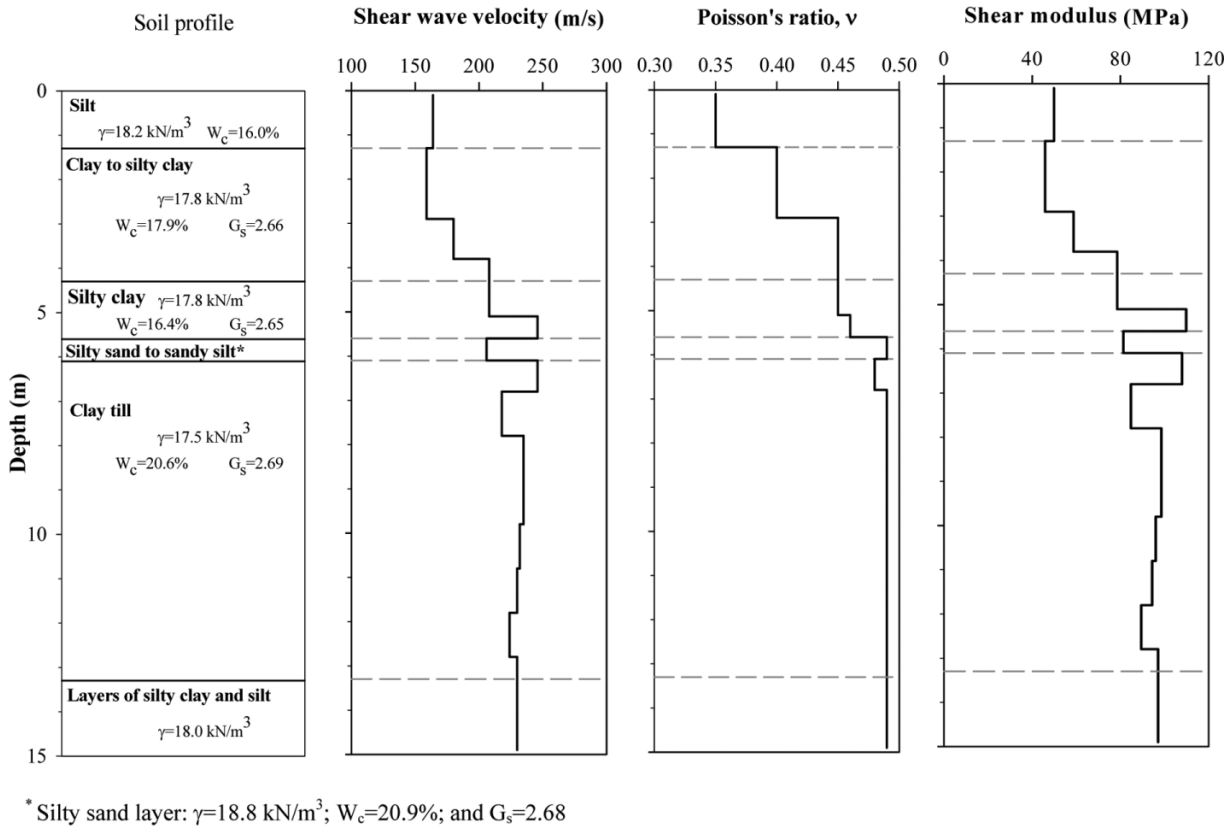

* Silty sand layer: γ=18.8 kN/m^3; W_c=20.9%; and G_s=2.68

Table 1. Properties of the test piles.

Property	Value
Outer shaft diameter (m)	0.324
Inner shaft diameter (m)	0.305
Moment of inertia (m^4)	1.164×10^{-4}
Cross-sectional area (m^2)	9.4102×10^{-3}
Pile length (m)	9.0
Helix plate diameter (m)	0.61
Helix plate thickness (m)	0.019
Young's modulus (GPa)	210
Poisson's ratio	0.3
Damping ratio	0.01
Unit weight (kN/m^3)	78.46
Coefficient of rigidity	1.11

frequency. Two uniaxial accelerometers were mounted on the test body at equidistant positions from the foundation centre on the axis of symmetry. The triaxial accelerometer was mounted on one side of the test body, at the elevation of the centre of gravity. The displacement responses derived from the three accelerometers were averaged to eliminate the rocking-mode component. To monitor the strain and force distribution along the helical pile, half-bridge strain gauge circuits were affixed on the inner wall of the pile at specified locations. Each level of gauges encompassed four half-bridges allocated equidistantly from each other as schematically shown in Fig. 5. To affix strain gauges on the inner surface of the pile shaft, the pile was cut into short segments. The gauges were installed at an approximate distance of 250 mm from the edge of each segment and then gauges and wires were covered with fibre cloth and epoxy. The pile's segments were then welded together to form the test pile.

Vertical vibration tests

The dynamic experiments were conducted first on the helical and driven piles 2 weeks after installation (case 1), when the soil around the pile shaft was disturbed because of the pile installation process. The vibration tests were then repeated on the helical pile 9 months after installation (case 2) to allow the disturbed soil to regain some of its original stiffness and strength. Consequently, the effect of the soil thixotropic behaviour on the dynamic performance of the helical pile could be analyzed. Initially, low excitation intensity was applied to the pile to keep the vibration amplitudes small enough to avoid any pile–soil separation or strong nonlinearity. The oscillator was derived to cover a frequency spectrum from about 3 to 60 Hz. The steady-state acceleration time history was recorded after reaching equilibrium by stopping enough times at each frequency.

For the adopted static mass — 4849.5 kg including the weight of cap, test body, and oscillator — tests were conducted at five different excitation intensities (0.091, 0.12, 0.16, 0.18, and 0.21 kg·m) for the helical pile and three intensities (0.091, 0.16, and 0.21 kg·m) for the driven pile. The excitation intensities are given in terms of $m_e e$ in which m_e and e are the oscillator eccentric rotating masses and the eccentricity of the rotating masses, respectively. The magnitude of the dynamic force, P_d, generated at the pile head is related to the excitation intensity of the oscillator and the measured acceleration by $P_d = m_e e\omega^2 \sin\omega t + ma$, where ω is the circular frequency, t is time, a is the measured acceleration at the centre of gravity of the cap-test body-oscillator assembly, and m is the static mass. The steady-state dynamic response to the induced vertical excitation was measured over the oscillator frequency range for the assigned excitation intensities.

Dynamic response of piles

The typical vertical vibration response curves for both the helical pile and the driven pile, measured under the effect of har-

Fig. 5. Schematic diagram of the test setup.

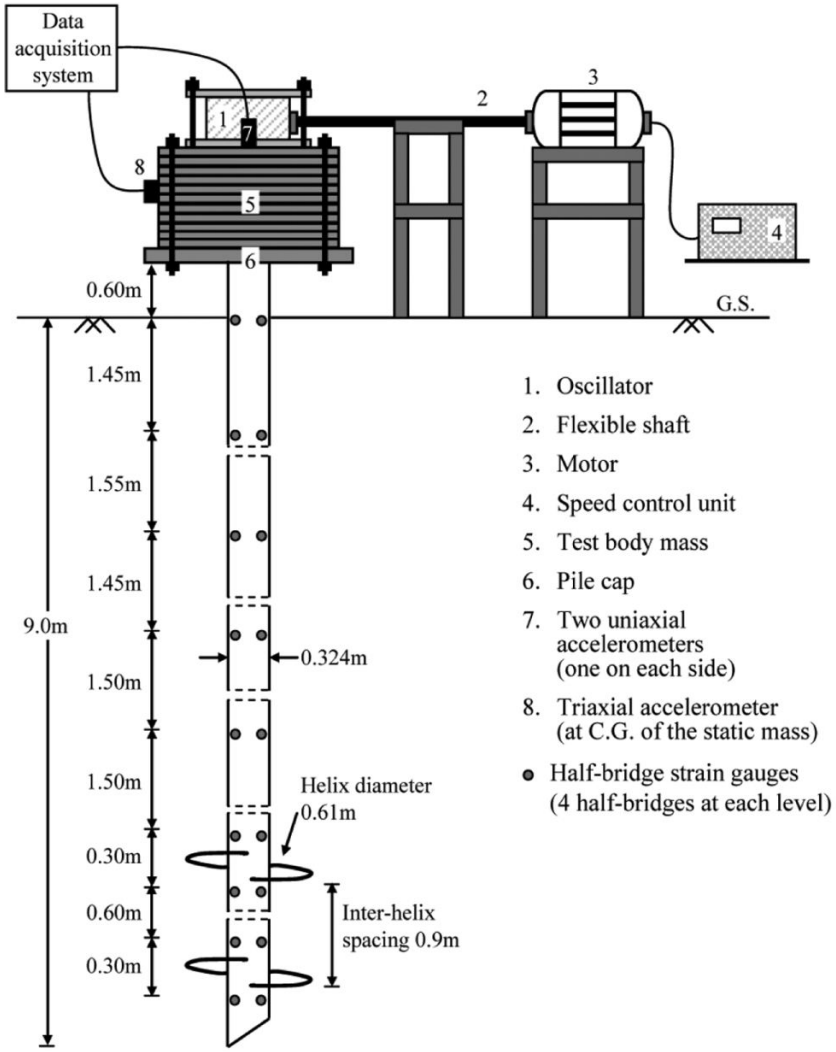

Table 2. Properties of test body, oscillator, and pile cap.

Properties	Value
No. of plates	59
Mass of cap, test body, and oscillator (kg)	4849.5
Height of centre of gravity (C.G.), Z_c (m)[a]	0.7911
Height of excitation above centre of gravity (C.G.), Z_e (m)	0.8606

[a]Height of C.G., Z_c, is measured from the bottom surface of the pile cap plate, which is located at 0.6 m above ground surface.

monic excitation of different intensities, are presented in Figs. 6*a*–6*c*. The displacement amplitudes were computed in three steps: base line correction, filtering, and double integration. In the first step, the acceleration time history was baseline-corrected using cubic polynomial-type correction to force the acceleration records to oscillate about zero. Step two involved using the Butterworth bandpass filter to suppress all noise frequencies in the acceleration record. A Fast Fourier Transform (FFT) analysis was then applied to the filtered record to obtain the dominant response frequencies to verify its closeness to the excitation frequency. In step three, a double integration process was performed using Simpson's rule to compute the displacement time history.

Vertical displacements of the piles vary with frequency and indicate a single resonant peak in all cases. The maximum (peak) displacement amplitudes measured at the centre of gravity of the static mass are 0.4 mm for the helical pile tested 2 weeks after installation (case 1), 0.31 mm for the same pile tested 9 months after installation (case 2), and 0.32 mm for the driven pile (case 1). These amplitudes reflect the relatively moderate level of applied vertical vibration. It is observed that as the excitation intensity increased, the measured response increased. The effect of soil thixotropy in the disturbed annular soil zone formed around the helical pile shaft during pile installation was studied. It is observed that resonant frequencies increased by 16% to 26% and resonant amplitudes decreased by 22% to 55%, based on the excitation intensity level, when the test was repeated 9 months after installation (case 2). This implies that both the stiffness and damping of the helical pile were increased with elapsed time after installation as a result of the improvement in stiffness and strength of the disturbed structured soil. On the other hand, the response of the driven pile (case 1) was very close to that of helical pile (case 1). This indicates that most of the soil reactions to dynamic vibration were developed along the pile shaft, as explained later in the paper. The observed differences in amplitudes may be ascribed to the variation of soil profile surrounding the pile and (or) the extent to which the soil was disturbed around the pile during installation.

Figures 7*a*–7*c* show the dimensionless response curves of the test piles. The dimensionless amplitudes are defined as $(m/m_e e)V$, where V is the measured vertical amplitude. For a linear vibrating

Fig. 6. Experimental vertical response curves: (*a*) helical pile, case 1; (*b*) helical pile, case 2; (*c*) driven pile, case 1.

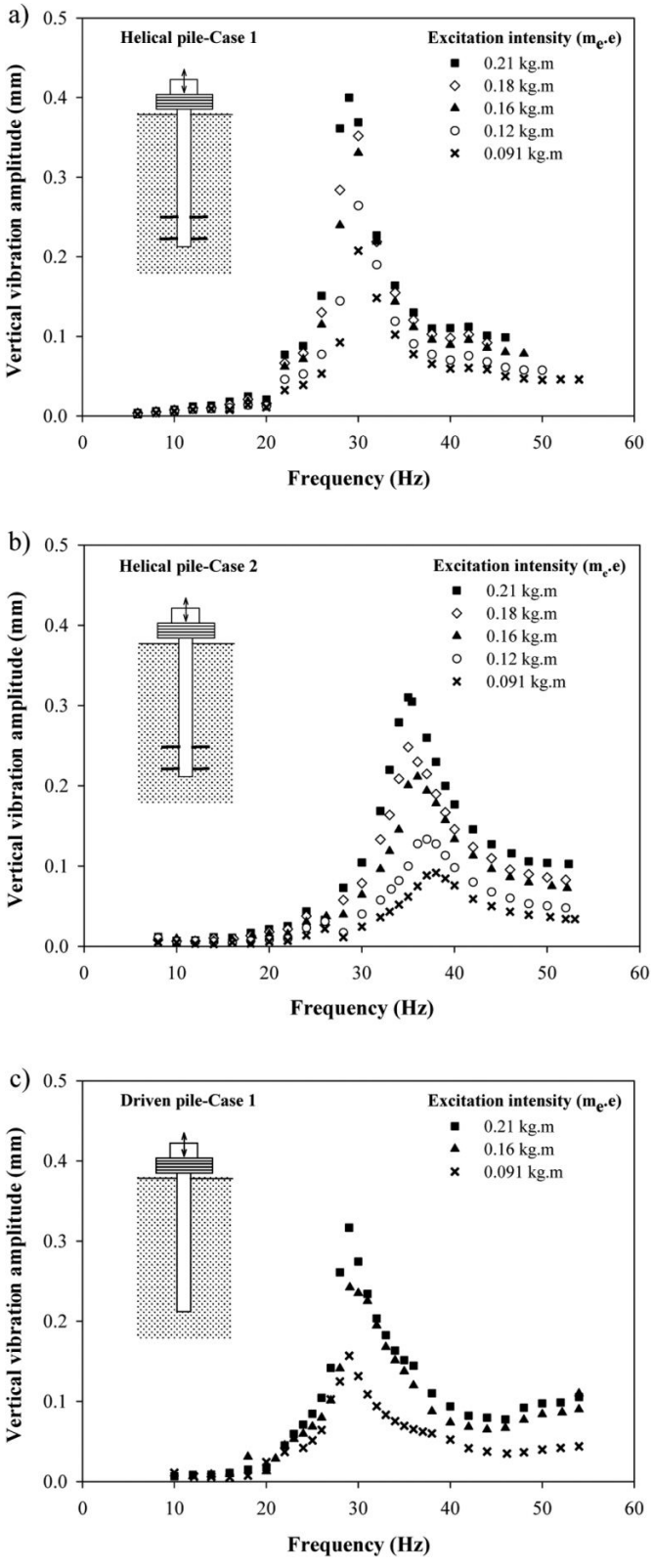

Fig. 7. Experimental dimensionless vertical response curves: (*a*) helical pile, case 1; (*b*) helical pile, case 2; (*c*) driven pile, case 1.

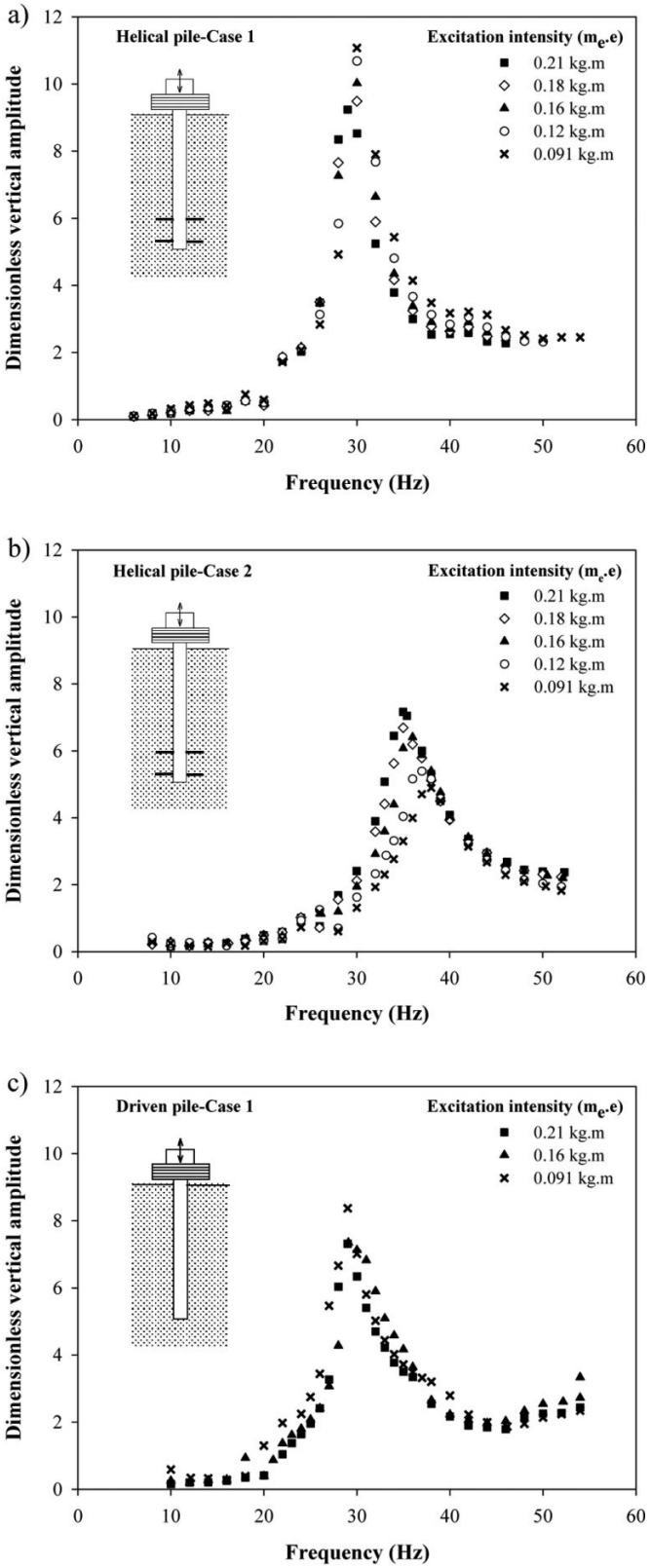

system, all dimensionless response curves for different excitation intensities should collapse onto one curve and the amount by which they differ represents the degree of the response nonlinearity. The nonlinearity is manifested by the reduction of the resonant frequency with the increase of excitation intensity. For the test piles, slight nonlinearity is observed, especially for the helical pile (case 2) where the measured resonant frequency shifts from 38 Hz for the lower excitation intensity to 35 Hz for the

Table 3. Experimental and theoretical results.

	Helical pile (case 1)		Helical pile (case 2)		Driven pile (case 1)	
$m_e e$ (kg·m)	f_{res} (Hz)	V_{res} (mm)	f_{res} (Hz)	V_{res} (mm)	f_{res} (Hz)	V_{res} (mm)
Experimental results						
0.091	30.0	0.208	38.0	0.092	29.0	0.157
0.12	30.0	0.264	37.0	0.134	—	—
0.16	30.0	0.331	36.0	0.211	29.0	0.242
0.18	30.0	0.351	35.0	0.248	—	—
0.21	29.0	0.400	35.0	0.310	29.0	0.317
Linear approach						
0.091	52.0	0.051	52.0	0.051	52.0	0.050
0.12	52.0	0.067	52.0	0.067	—	—
0.16	52.0	0.090	52.0	0.090	52.0	0.089
0.18	52.0	0.101	52.0	0.101	—	—
0.21	52.0	0.118	52.0	0.118	52.0	0.116
Nonlinear approach						
0.091	30.9	0.192	38.0	0.104	30.3	0.146
0.12	30.8	0.244	37.2	0.141	—	—
0.16	30.5	0.319	36.2	0.198	30.3	0.259
0.18	30.4	0.353	35.4	0.248	—	—
0.21	30.0	0.397	35.1	0.300	30.3	0.340

Note: $m_e e$, excitation intensity; f_{res}, resonant frequency; V_{res}, resonant amplitude.

higher intensity. This indicates a reduction in stiffness (which is proportional to square of frequency) of almost 16% compared to the highest value, associated with the lowest excitation intensity. The experimental test results including resonant frequencies, f_{res}, and amplitudes, V_{res}, at the adopted excitation intensities are summarized in Table 3.

Theoretical analysis

The response of piles to dynamic loads is largely affected by the interaction between the piles and the surrounding soil. This interaction modifies the stiffness of the piles and generates geometrical and hysteretic damping. Two different theoretical continuum approaches were adopted to investigate the performance of both of the helical pile and driven pile under harmonic vertical vibrations. This includes estimation of the response curves, dynamic load in piles, and stiffness and damping of the pile–soil system. The two approaches are incorporated in the computer program DYNA 6 (El Naggar et al. 2011).

Linear approach

The theoretical approach was presented by Novak and Aboul-Ella (1978*a*, 1978*b*) using the plane strain condition as an extension of the elastic solution provided by Baranov (1967) and Novak (1974, 1977). The approach was used to derive the impedance functions (stiffness and damping) of piles in a layered soil medium. The main assumptions adopted in the theoretical formulation are: (*i*) the soil is composed of horizontal linearly viscoelastic layers with hysteretic material damping; (*ii*) the pile is elastic and divided into finite elements, each of the same length as the side soil layer; and (*iii*) the soil below the pile toe is a viscoelastic half-space. The soil reactions to pile vertical vibration were provided in terms of complex soil stiffness by Novak et al. (1978) for soil reaction along the pile shaft (eq. [3]) and by Veletsos and Verbič (1973) for soil reaction at the pile toe (eq. [4]), as follows:

$$(3) \qquad k_{vs} = G_{os}(S_{v1} + iS_{v2})$$

$$(4) \qquad k_{vt} = G_{ot}R_t(C_{v1} + iC_{v2})$$

where G_{os} and G_{ot} are the shear modulus of soil along pile shaft and toe, respectively; S_{v1} and S_{v2} are the real and imaginary parts, respectively, of the dimensionless complex soil stiffness along pile shaft; $i = \sqrt{-1}$; R_t is the pile toe radius; and C_{v1} and C_{v2} are the real and imaginary parts, respectively, of the dimensionless complex soil stiffness at pile toe. With harmonic motion having complex amplitude, the complex frequency-dependent impedance at the pile head is expressed as

$$(5) \qquad K_v = k_{v1} + ik_{v2}$$

where k_{v1} and k_{v2} are the dynamic stiffness and damping impedances, respectively. The notation k_{v2} is equivalent to ωc, where c is the equivalent viscous damping coefficient that accounts for geometric and hysteretic damping.

Nonlinear approach

The pile performance may be affected by the remoulding of soil around the pile during installation, nonlinearity of soil at the zone of high strain, lack of bond at the pile–soil interface, slippage, and separation. To account for most of these factors, Novak and Sheta (1980) extended the plane strain theory to assume that the pile is surrounded by a linear viscoelastic medium composed of two zones: an outer zone and an inner cylindrical weakened boundary zone surrounding the pile, as presented in Fig. 8. Soil disturbance and nonlinearity, weakened bond, and slippage are accounted for by a reduced shear modulus and increased material damping of the weakened boundary zone of soil. The parameters characterizing the properties of the weakened zone, including the shear modulus ratio, G_m/G_o; damping ratio, D_m; thickness, t_m; and mass participation factor (M.P.F.) assigned to represent the percentage of weak-zone soil mass vibrating in-phase with the pile, play an appreciable role in the overall dynamic response of the piles.

The complex soil reactions of the composite medium were developed by Novak and Sheta (1980) and substituted into the approach presented by Novak and Aboul-Ella (1978*a*) to calculate the complex and frequency-dependent stiffness and damping constants of the piles, as follows:

$$(6) \qquad K_{vm} = k_{vm1} + ik_{vm2} = \frac{E_p A}{R}\left(f_{vm1} + i\frac{\omega R}{V_t}f_{vm2}\right)$$

where K_{vm} is the total stiffness of pile in the composite medium; k_{vm1} and k_{vm2} are the stiffness and damping impedances, respectively; E_p and A are the modulus of elasticity and cross-sectional area of the pile, respectively; R is the pile shaft radius; f_{vm1} and f_{vm2} are the dimensionless stiffness and damping parameters, respectively; and V_t is the shear wave velocity near the pile toe. It is worth mentioning that this approach does not account for pile–soil separation near ground surface, which instead could be modeled in DYNA 6 as a void soil layer with $G_o = 0$.

Theory versus experiments

To develop the theoretical results, the pile (helical or driven) was divided into a number of elements corresponding to the adjacent soil layers with different shear wave velocities. By using the relevant pile and soil properties shown in Fig. 4 and Tables 1 and 2, and assigning a layered soil profile, the vertical response of the test piles was obtained. For the case of the helical pile, an idealization was made in the program DYNA 6 to model the helices attached to the pile, in which the two helices were modelled as one helix, of the same area, attached to the end of the helical pile. As shown by Novak (1977) and Novak and El Sharnouby (1983), the pile toe condition has significant influence on the dynamic response. In the current analysis, the toe condition of the helical pile as well as the driven pile suggests that the test piles behaved as floating piles.

Fig. 8. Schematic diagram for the nonlinear analysis model. *D*, material damping; *t*, weak-zone thickness; ρ, density; ν, Poisson's ratio; subscript m denotes inner soil zone.

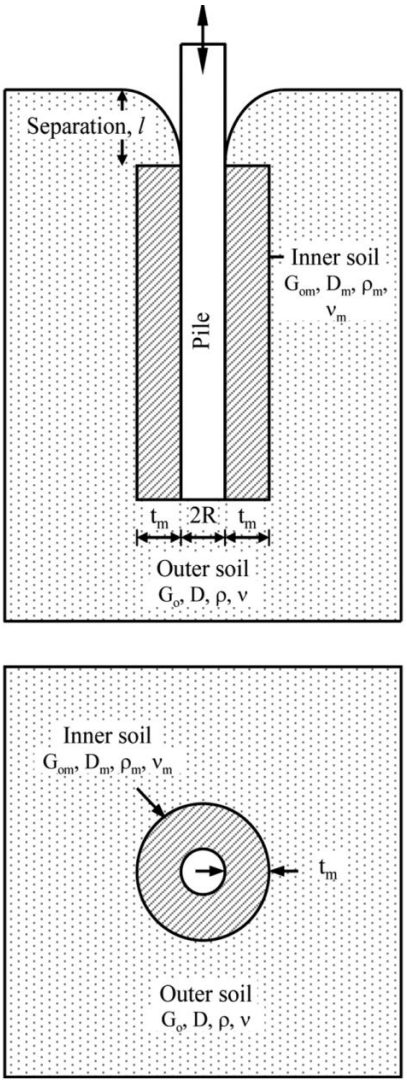

Fig. 9. Experimental versus linear approach response curves: (*a*) helical pile, case 1; (*b*) helical pile, case 2; (*c*) driven pile, case 1.

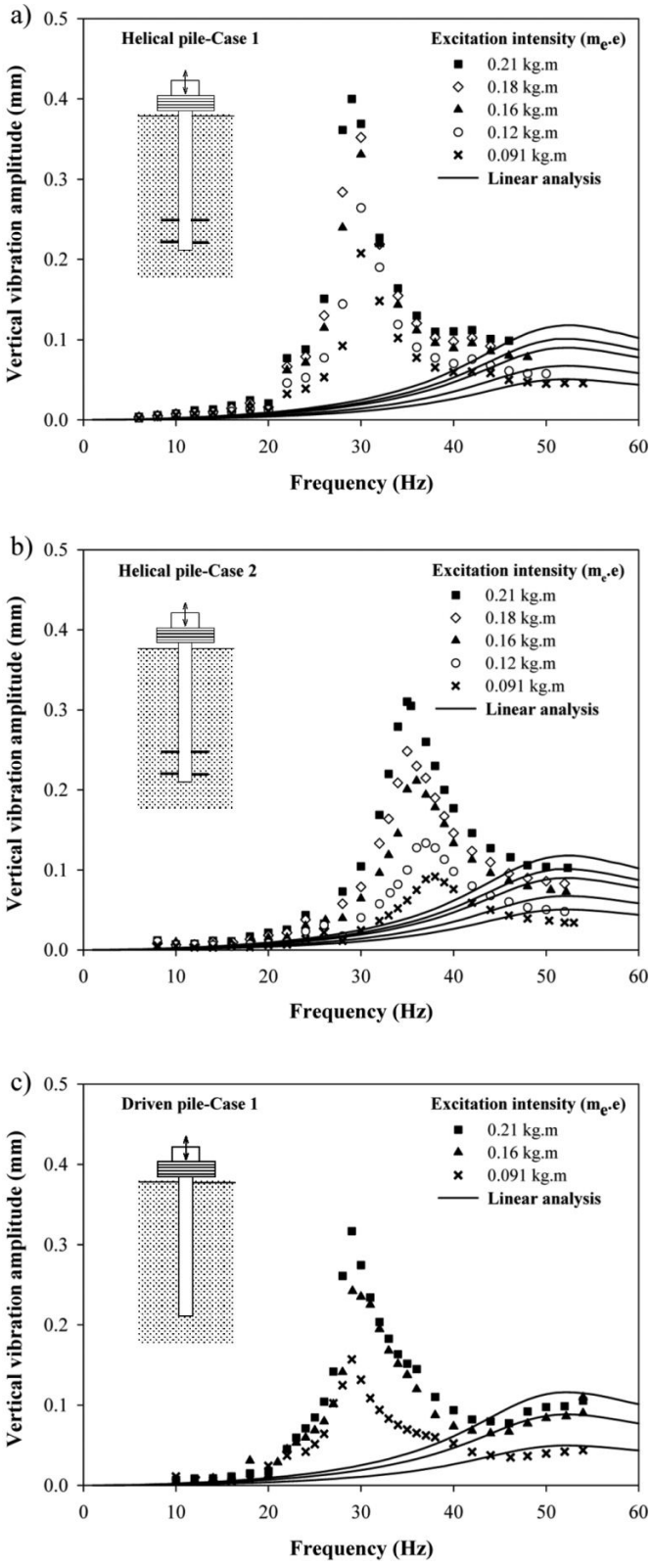

Comparison with linear approach

In this analysis, no weak zone around the pile was considered and the value of the damping ratio of soil was assumed constant (5%) with depth. The soil beneath the toe of the helical pile was assumed to be homogeneous with an average shear modulus that represents the undisturbed soil beneath the upper and lower helices. The calculated response assuming no change of soil properties due to installation, i.e., no soil disturbance, (and denoted here as linear analysis) are compared with the measured response curves in Figs. 9*a*–9*c*. By inspecting figures, it can be noted that there are significant differences between the calculated and measured response curves. The natural frequencies estimated from the linear approach are much higher than the measured values, by an average of 73% for helical pile (case 1) and driven pile (case 1). However, for the second phase of testing (helical pile (case 2)), the difference decreased to about 40%. In addition, the estimated resonant peaks are more rounded, indicating higher damping compared to the experimental results. This is also indicated in terms of much lower calculated vibration amplitudes compared to the measured values. The theoretically calculated values of stiffness were found to be higher than the experimental results by 145% for helical pile (case 1) and driven pile (case1) and by 62% to 88% for helical pile (case 2).

These discrepancies are attributed to the fact that the soil adjacent to the test piles was disturbed due to the installation process.

Such disturbance is confined to an annular zone around the pile, and leads to remoulding of the soil and imperfect contact at the pile–soil interface. This effect is not accounted for in the linear approach. Ignoring soil disturbance in the analysis leads to an overestimation of the resonant frequency and damping and an underestimation of the resonant amplitude. With the passage of time, the soil regains its strength and eventually the expected behaviour matches that determined considering the linear (undisturbed) soil conditions.

The disturbance that occurred around the helical pile is believed to be highly significant. This is attributed to the nature of structured cemented silty clay – clayey silt soils encountered at the test site. The installation disturbance destroyed the cementation between the soil particles, which may require a long time to be re-established. Similar effects are expected to occur for the driven pile due to the disturbance associated with the driving process. O'Neill (2001) recommended that the capacity of driven piles in silty clay and clayey silt be reduced by 50% because of the installation effects. He theorized that due to the propagation of stress waves during pile driving, the pile shaft vibrates, pushing the soil away from the shaft and thus reducing the contact surface (imperfect bonding between pile and soil). This level of disturbance is not expected to occur in sandy soils or normally consolidated cohesive soils. Consequently, the linear approach is not considered the ideal methodology to predict the post-installation vertical vibration response of helical and driven piles installed in silty clay and clayey silt till.

Comparison with nonlinear approach

To properly estimate the behaviour of test piles considering the effects of soil disturbance, soil nonlinearity, and pile–soil separation, the nonlinear approach is adopted to account for radial soil inhomogeniety. Randolph et al. (1979) concluded that the zone of soil disturbance around driven piles installed in clayey soils extends 1 to 2 times the pile radius due to changes in the state of stresses and pore pressure. For helical piles, it is expected that the zone of soil disturbance would be slightly larger than the helix diameter. A constant ratio of weak zone thickness to pile shaft radius, $t_m/R = 1.2$, is assumed for both helical and driven piles.

The soil parameters in the weak boundary zone (especially the most influential parameters, G_m/G_o and D_m) were obtained through a trial-and-error technique to achieve a reasonable match between the calculated and measured response curves. The characteristics of the weak zone parameters for different excitation intensities are given in Figs. 10*a*–10*c* and Table 4. It can be noted that as the excitation intensity increases, the shear modulus ratio, G_m/G_o, is reduced whereas the material damping ratio, D_m, is increased. This can be observed in helical pile cases 1 and 2, where slight to moderate soil nonlinearity is monitored. The ratio of G_m/G_o is assumed to increase with depth, but D_m decreases with depth (i.e., the soil disturbance and nonlinearity are less for deeper soils). The elapsed time of 9 months between the dynamic test of helical pile cases 1 and 2 had a significant effect on the stiffening properties of the weak zone. Inspecting Figs. 10*a* and 10*b*, it is observed that the G_m/G_o ratio increased from the first to second round of dynamic testing by 100% to 345%, depending on excitation intensity. Thus, the soil is expected to continue to regain stiffness and eventually the pile stiffness (and response) will approach the values predicted by the linear analysis.

The weak zone's Poisson's ratio, ν_m, is taken 0.3 and is assumed to be constant with depth. The mass of the weak zone, neglected in the zone stiffness and damping evaluation to avoid wave reflections and refractions from the fictitious interface between the weak zone and the outer intact soil zone, can be added in full or in part to the mass of the pile. To account for the fraction of the weak zone mass to be added to the pile, a mass participation factor, M.P.F., is introduced in the model. Not to exaggerate its effect, it should be chosen as less than 1.0 (i.e., between 0 and 1.0), and decreasing with the increase in excitation intensity (i.e., increase

Fig. 10. Distribution of the weak zone shear modulus ratio, G_m/G_o, and material damping, D_m, with depth: (*a*) helical pile, case 1; (*b*) helical pile, case 2; (*c*) driven pile, case 1.

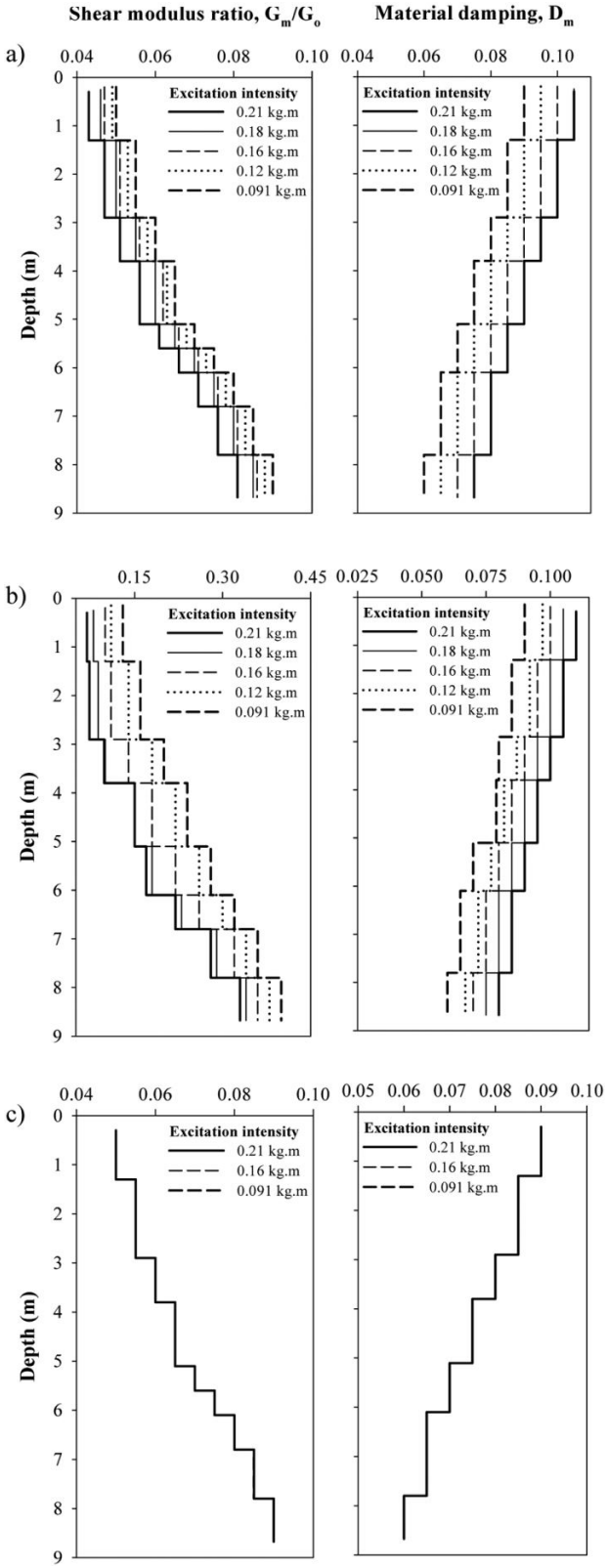

Table 4. Nonlinear approach parameters.

	Helical pile (case 1)			Helical pile (case 2)			Driven pile (case 1)		
$m_e e$ (kg·m)	l (m)	M.P.F.	D.S.F.	l (m)	M.P.F.	D.S.F.	l (m)	M.P.F.	D.S.F.
0.091	0.20	0.25	1.55	0.15	0.60	1.0	0.30	0.25	1.02
0.12	0.20	0.25	1.50	0.15	0.60	1.0	—	—	—
0.16	0.20	0.25	1.50	0.20	0.55	1.0	0.30	0.25	1.02
0.18	0.25	0.25	1.45	0.25	0.40	1.0	—	—	—
0.21	0.30	0.25	1.45	0.30	0.35	1.0	0.30	0.25	1.02

Note: l, pile–soil separation length; M.P.F., mass participation factor; D.S.F., damping safety factor.

in nonlinearity in response). The estimated values for M.P.F. were inferred by using a trial-and-error technique for matching the theoretical and measured response curves. An M.P.F. value of 0.25 is considered for case 1 for both the helical and driven piles, while a higher M.P.F. is assumed to decrease with excitation intensity for helical pile (case 2). The higher M.P.F. values reflect the fact of the regained soil stiffness and strength with time. On the other hand, the properties of the soil medium surrounding the weak zone are similar to those given in the linear approach. As the level of applied excitation was slight to moderate, it was considered that the pile separation adopted in the analysis was developed mainly during the installation. However, obtaining reliable values for pile–soil separation by physical measurements at ground surface was difficult. A trial-and-error technique was employed in the analysis and different separation values, l, were adopted until reaching the optimum. A ratio of $G_m/G_o = 0$ is assigned for the topmost layer to account for the pile–soil separation in the analysis. The estimated depth of separation ranges between 0.92R (0.15 m) and 1.85R (0.3 m) for the test piles.

The calculated vertical dynamic responses of the test piles using the nonlinear approach properties as explained above are plotted versus the experimental results in Figs. 11*a*–11*c*. It is observed that there is a favourable agreement between the measured and calculated responses using the nonlinear approach. It can be concluded that it is necessary to incorporate the weak boundary zone and pile–soil separation in the model to better match the real vertical vibration performance of helical and driven piles in terms of resonant frequencies, amplitudes, and damping. A comparison between the measured and calculated results using both linear and nonlinear approaches is given in Table 3.

Distribution of dynamic load in pile

The distribution of dynamic load along the helical pile during the vertical vibration test was evaluated from the strain measurements recorded at different strain gauge stations along the pile. The distribution of these loads represents the load transfer to the soil, and helps to understand the behaviour of the helical pile under dynamic loads. It is worth noting that no strain gauges were affixed on the driven pile's shaft. Figures 12*a* and 12*b* illustrate the distribution of vertical dynamic load with depth for helical pile cases 1 and 2, respectively. The figures demonstrate clearly that the dynamic load was transferred to surrounding soil through shaft resistance, with insignificant influence from the helices. Also, it is observed that most of the dynamic load in the helical pile (75% of the load) has been transferred along the upper 6.0 m of the shaft, which can be considered as the effective length of the tested pile. In the current study, it should be noted that the induced level of excitation was mainly moderate.

The nonlinear model established using DYNA 6 was employed to calculate the distribution of dynamic load along the helical and driven piles. A comparison between the measured and calculated distribution of the dynamic load in the helical pile is illustrated in Figs. 12*a* and 12*b*, while Fig. 12*c* presents the calculated distribution in the driven pile. In most cases, there are favourable matches between the measured and calculated curves except near the lower part of the helical pile, as the nonlinear approach overestimates the load values in the pile. This can be ascribed to the

Fig. 11. Experimental versus nonlinear approach response curves: (*a*) helical pile, case 1; (*b*) helical pile, case 2; (*c*) driven pile, case 1.

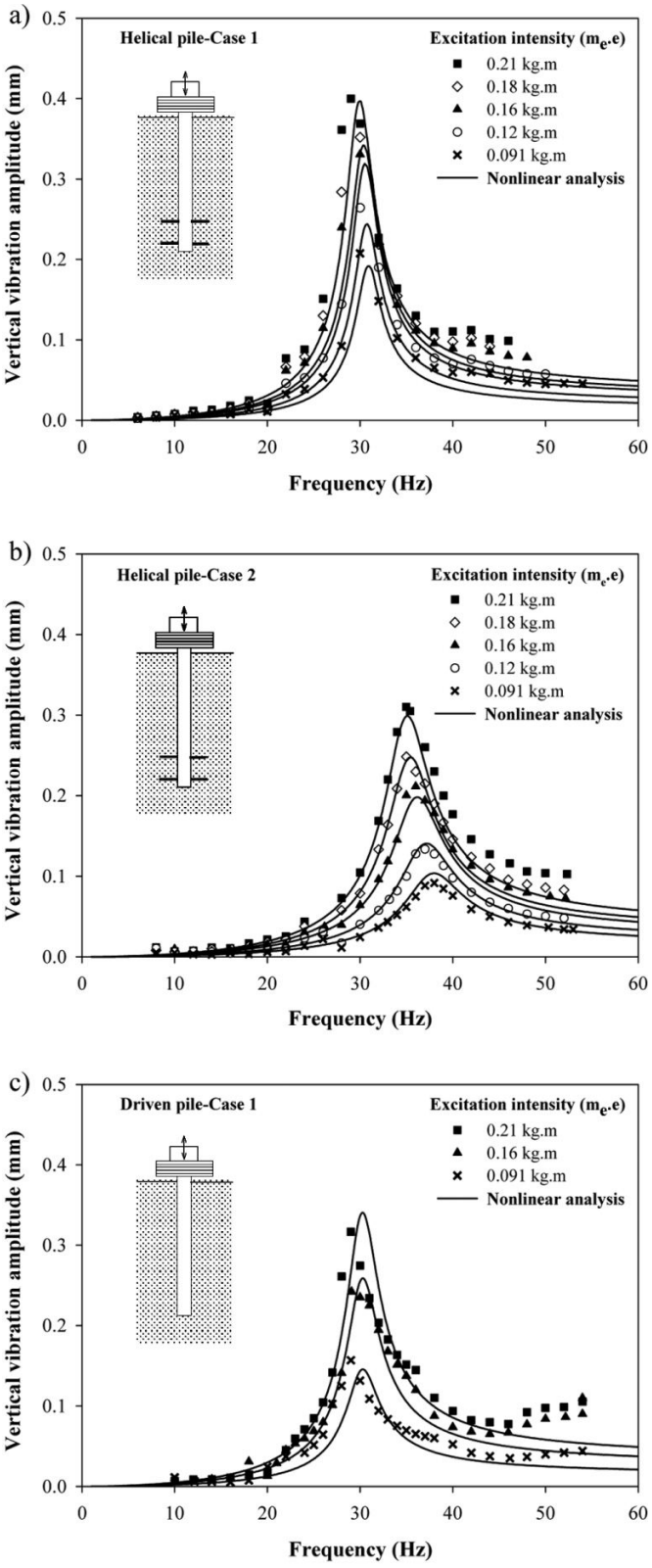

Fig. 12. Experimental versus nonlinear approach load distribution in pile: (*a*) helical pile, case 1; (*b*) helical pile, case 2; (*c*) driven pile, case 1.

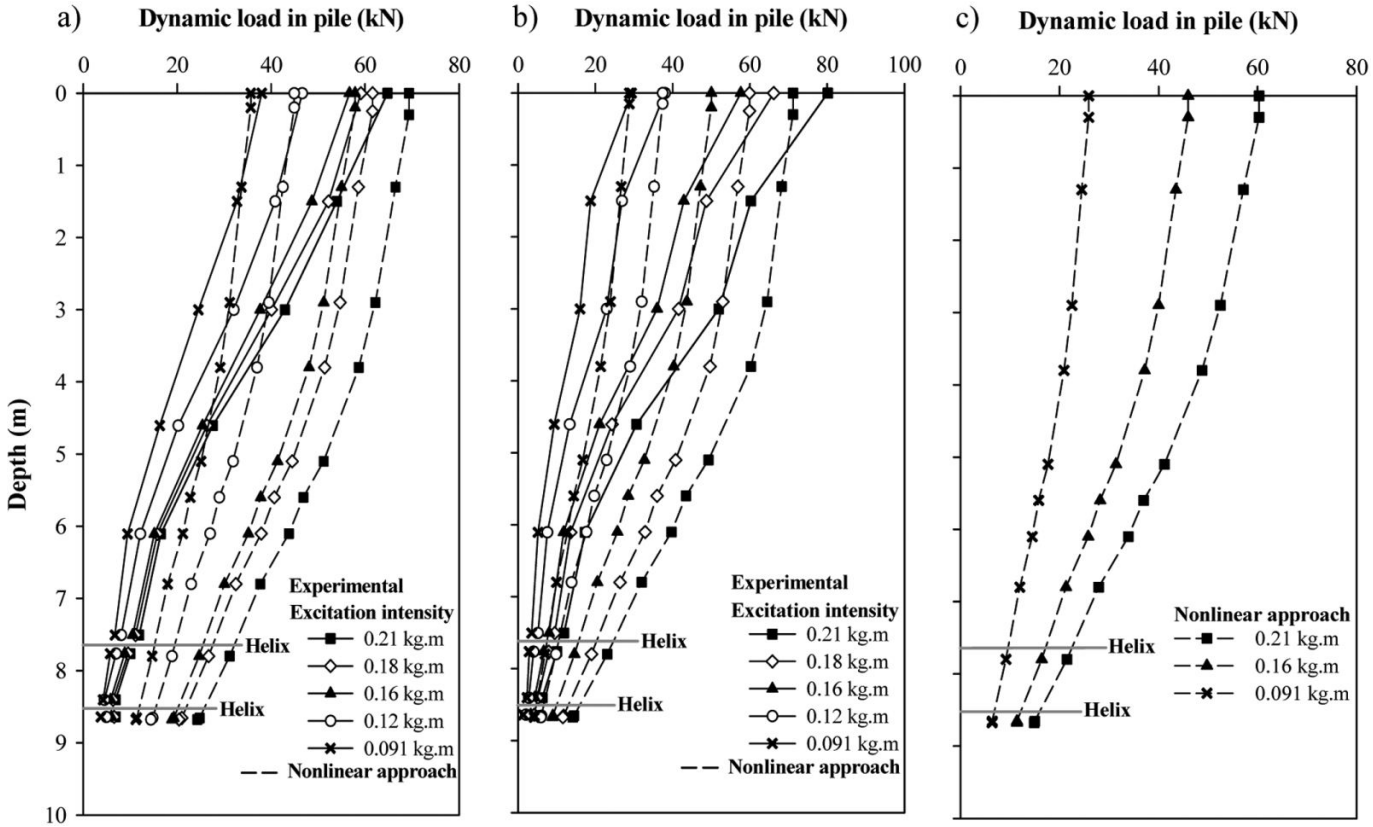

fact that the nonlinear approach assumes full mobilization of both the soil reactions along the pile shaft and at the pile toe. Thus, the idealized helix at the pile toe, in the nonlinear model, directs a portion of the dynamic load to be transferred to soil by end bearing. Furthermore, the effect of the mobilized compression residual stresses at the end of the pile installation are believed to be an additional cause for such discrepancy between measured and calculated distribution of dynamic load near the lower part of the pile, as the pile was considered "stress-free" before starting the dynamic tests.

Pile stiffness and damping

The theoretical pile head vertical stiffness and damping, calculated from the linear and nonlinear approaches, for the three adopted cases — named helical pile (case 1), helical pile (case 2), and driven pile (case 1) — are shown in Figs. 13*a*–13*c*. The figures show that the linear approach highly overestimates both the stiffness and damping of piles, and as expected, they have same stiffness and damping characteristics for different excitation intensities.

Also, it is noticed that the stiffness is not sensitive to frequency changes, especially at low frequencies. This is attributed to the fact that at a low frequency the dynamic stiffness of the pile is quite close to the static stiffness. However, the damping coefficient of the piles increases rapidly as the frequency approaches zero, as a result of converting the soil material damping to the frequency-dependent equivalent viscous damping coefficient, *c*. For curves predicted by the nonlinear approach, helical pile (case 2), it is concluded that the stiffness decreases as the excitation intensity increases; however, for helical pile (case 1) and driven pile (case 1), the stiffness remains almost constant over the range of applied excitation. This emphasizes the observation that the only case that has a nonlinear response is helical pile (case 2). Furthermore, it is noticed that the damping coefficient, for helical pile (case 2), decreases with the increase of excitation intensity. Although this appears contrary to the usual trend, it is a consequence of soil-softening in the weak zone and the development of pile separation as the excitation intensity is increased, which results in a reduction of the geometrical damping of the system. Comparing cases 1 and 2 of the helical pile, it is observed that the average increases in stiffness and damping are about 42% and 90%, respectively, as a result of soil stiffness and strength gain in the weak zone with elapsed time after pile installation.

Summary and conclusions

This study investigated the in situ dynamic performance of two full-scale, large-capacity helical and driven piles. The experimental results were used to verify the applicability of the plane strain theoretical formulations to the prediction of stiffness and damping of helical and driven piles, and to evaluate their response to harmonic loading. Also, the effect of soil disturbance and thixotropic behaviour of soil around the helical pile on the dynamic response as well as the dynamic load transfer mechanism were investigated. The field tests included a closed-ended, double-helix, large-diameter helical pile of 9.0 m length, 0.324 m shaft diameter, and 0.61 m helix diameter, as well as a closed-ended, driven steel–pipe pile with the same length and diameter. The piles were installed in Ponoka, Alberta, Canada. Several tests with different excitation intensities were performed. The helical pile was tested twice; once 2 weeks after installation, and another after 9 months. The driven pile was tested 2 weeks after installation. In total, 13 vertical harmonic vibration tests were conducted. Two different theoretical approaches were conducted based on the continuum approach; namely, linear and nonlinear approaches, incorporated in the program DYNA 6. The analytical solutions were used to calculate the dynamic characteristics and response curves of the piles considered in the experimental program. The nonlinear approach accounted for the weak boundary zone and pile–soil sepa-

Fig. 13. Vertical stiffness and damping of piles: (*a*) helical pile, case 1; (*b*) helical pile, case 2; (*c*) driven pile, case 1.

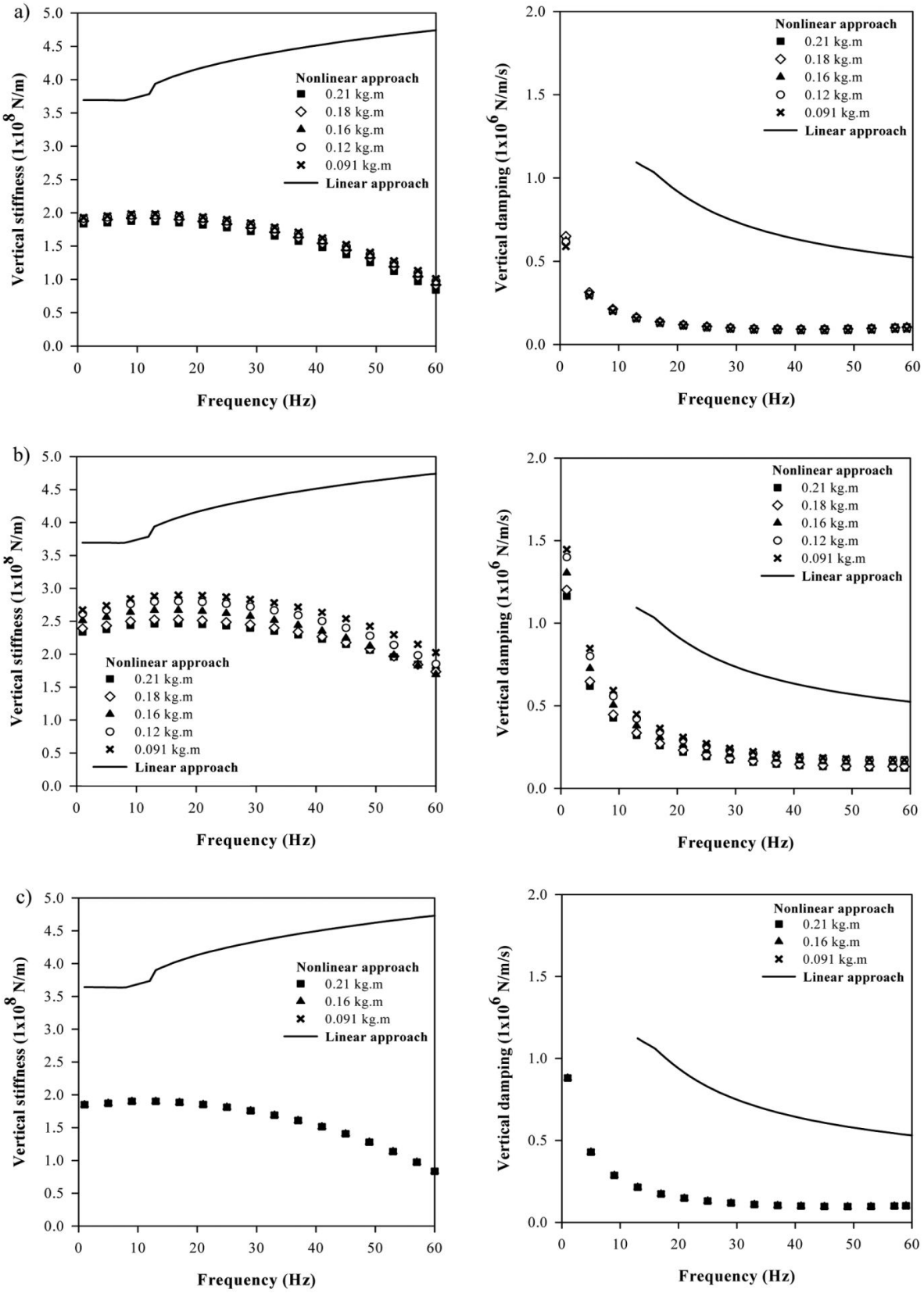

ration. Based on the experimental and analytical results obtained in this study, the following conclusions can be drawn:

1. The consistency of the measured test datasets confirmed the accuracy of the measured data and the suitability of the interpretation procedure. The measured response curves showed slight to moderate nonlinearity in the helical pile's response, which was manifested by a reduction in the resonant frequency with increasing excitation intensity.
2. The measured responses of the driven pile were significantly close to those of the helical pile tested 2 weeks after installation. This demonstrates that the performance characteristics of large-capacity helical piles are similar to those of closed-ended steel driven piles for the piles' geometry considered in this study.
3. The field measurements of the vertical dynamic load distribution along the helical pile showed insignificant influence of the helices on the load transfer mechanism and that the dynamic load was transferred to the surrounding soil medium mainly through the interface resistance between pile shaft and soil.
4. The theoretical analysis based on the linear approach highly overestimated both the stiffness and damping of the piles due to the assumed perfect bonding between pile and soil. The theoretically calculated values of stiffness were found to be higher than the experimental results by 145% for the helical pile and driven pile tested 2 weeks after installation and by 62% to 88% for the helical pile tested 9 months after installation.
5. The theoretical analysis based on the nonlinear approach provided a reasonable estimation for the piles' response curves and impedance parameters. Such agreement, achieved by considering a weak boundary zone around the pile, confirmed the influence of soil disturbance, due to the pile installation process, on the dynamic response of helical and driven piles.
6. The nonlinear approach predicted an average increase of 42% in stiffness and of about 90% in damping for the helical pile after a 9 month period, due to the stiffening of soil within the weak zone with elapsed time after pile installation.
7. The pile–soil separation length predicted by the nonlinear approach for the helical and driven piles varied between 0.92 and 1.85 times the shaft radius, under the adopted levels of dynamic excitation.
8. The close agreement between the measured and calculated response curves validated the ability of existing tools to model the dynamic behaviour of helical piles. This will undoubtedly increase the confidence of design engineers to consider helical piles as a design option for applications involving dynamic loads.

It should be noted that these conclusions are based on a limited number of vertical dynamic tests on a single type of helical pile. It should also be noted that the experimental results are site-specific and must be used with caution when applied elsewhere. However, it is encouraging that the presented simplified nonlinear model in DYNA 6 can adequately simulate the dynamic vertical response of the above-mentioned helical and driven piles, and provide a practical tool for the dynamic analysis of these piles.

Acknowledgements

The research described herein received direct support from the Natural Sciences and Engineering Research Council of Canada, The University of Western Ontario, and ALMITA Manufacturing Ltd., Canada.

References

Adams, J.I., and Klym, T.W. 1972. A study of anchorages for transmission tower foundations. Canadian Geotechnical Journal, **9**(1): 89–104. doi:10.1139/t72-007.

Baldi, G., Belloti, R., Ghionna, V., Jamiolkowski, M., and LoPresti, D.C.F. 1989. *In* Proceedings of the 12th International Conference on Soil Mechanics and Foundation Engineering, Rio de Janeiro, Brazil, 13-18 August 1989. A.A. Balkema, Rotterdam, the Netherlands. Vol. 1. pp. 165–170.

Baranov, V.A. 1967. On the calculation of excited vibrations of an embedded foundation. Voprosy Dinamiki Prochnocti, Polytech. Institute Riga, **14**: 195–209.

Blaney, G.W., Muster, G.L., and O'Neill, M.W. 1987. Vertical vibration test of a full-scale pile group. *In* Proceedings of Specialty Session, ASCE Convention on Dynamic Response of Pile Foundations - Experiment, Analysis, and Observation. Atlantic City, N.J., 27 April 1987. Geotechnical Special Publication No. 11. ASCE, New York. pp. 149–165.

Bobbitt, D.E., and Clemence, S.P. 1987. Helical anchors: application and design criteria. *In* Proceedings of the 9th Southeast Asian Geotechnical Conference, Bangkok, Thailand, 7-11 December 1987. South East Asian Geotechnical Society, Hong Kong. Vol. 2. pp. 6-105–6-120.

Carville, C.A., and Walton, R.W. 1995. Foundation repair using helical Screw anchors. *In* Proceedings of the Symposium on Foundation Upgrading and Repair for Infrastructure Improvement, San Diego, Calif., 23-26 October 1995. Geotechnical Special Publication No. 50. ASCE, New York. pp. 56–75.

Dobry, R., Vicente, E., O'Rourke, M.J., and Roesset, J.M. 1982. Horizontal stiffness and damping of single piles. Journal of Geotechnical Engineering Division, ASCE, **108**(3): 439–459.

El Marsafawi, H., Han, Y.C., and Novak, M. 1992. Dynamic experiments on two pile groups. Journal of Geotechnical Engineering, **118**(4): 576–592. doi:10.1061/(ASCE)0733-9410(1992)118:4(576).

El Naggar, M.H., and Abdelghany, Y. 2007*a*. Seismic helical screw foundations systems. *In* Proceedings of the 60th Canadian Geotechnical Conference, Ottawa, Ontario, 21-24 October 2007. Canadian Geotechnical Society, B.C. Paper 160.

El Naggar, M.H., and Abdelghany, Y. 2007*b*. Helical screw piles (HSP) capacity for axial cyclic loadings in cohesive soils. *In* Proceedings of the 4th International Conference on Earthquake Geotechnical Engineering, Thessaloniki, Greece, 25-28 June 2007. ISSMGE. Paper 1567.

El Naggar, M.H., and Novak, M. 1992. Analytical model for an innovative pile test. Canadian Geotechnical Journal, **29**(4): 569–579. doi:10.1139/t92-064.

El Naggar, M.H., and Novak, M. 1994. Non-linear model for dynamic axial pile response. Journal of Geotechnical Engineering, **120**(2): 308–329. doi:10.1061/(ASCE)0733-9410(1994)120:2(308).

El Naggar, M.H., Shayanfar, M.A., Kimiaei, M., and Aghakouchak, A.A. 2005. Simplified BNWF model for nonlinear seismic response analysis of offshore piles with nonlinear input ground motion analysis. Canadian Geotechnical Journal, **42**(2): 365–380. doi:10.1139/t04-103.

El Naggar, M.H., Novak, M., Sheta, M., El Hifnawi, L., and El Marsafawi, H. 2011. DYNA 6 – a computer program for calculation of foundation response to dynamic loads. Geotechnical Research Centre, The University of Western Ontario, London, Ont.

El Sharnouby, B., and Novak, M. 1984. Dynamic experiments with group of piles. Journal of Geotechnical Engineering, **110**(6): 719–737. doi:10.1061/(ASCE)0733-9410(1984)110:6(719).

Elkasabgy, M., El Naggar, M.H., and Sakr, M. 2010. Full-scale vertical and horizontal dynamic testing of a double helix screw pile. *In* Proceedings of the 63rd Canadian Geotechnical Conference, Calgary, Alta., 12-16 September 2010. Canadian Geotechnical Society, B.C. pp. 352–359.

Kuhlemeyer, R.L. 1979. Vertical vibration of pile. Journal of Geotechnical Engineering Division, ASCE, **105**(2): 273–287.

Kuhlemeyer, R.L. 1981. Dynamic response curves for vertically loaded floating pile foundations. Canadian Geotechnical Journal, **18**(2): 300–312. doi:10.1139/t81-033.

Manna, B., and Baidya, D.K. 2009. Vertical vibration of full-scale pile - analytical and experimental study. Journal of Geotechnical and Geoenvironmental Engineering, **135**(10): 1452–1461. doi:10.1061/(ASCE)GT.1943-5606.0000110.

Mayne, P., and Rix, G.J. 1995. Correlations between shear wave velocity and cone tip resistance in natural clays. Soils and Foundations, **35**(2): 107–110. doi:10.3208/sandf1972.35.2_107.

Nogami, T., and Novak, M. 1976. Soil-pile interaction in vertical vibration. International Earthquake Engineering and Structural Dynamics, **4**(3): 277–293. doi:10.1002/eqe.4290040308.

Novak, M. 1974. Dynamic stiffness and damping of piles. Canadian Geotechnical Journal, **11**(4): 574–598. doi:10.1139/t74-059.

Novak, M. 1977. Vertical vibration of floating piles. Journal of the Engineering Mechanics Division, ASCE, **103**(EM1): 153–168.

Novak, M., and Aboul-Ella, F. 1978*a*. Impedance functions of piles in layered media. Journal of the Engineering Mechanics Division, ASCE, **104**(33): 643–661.

Novak, M., and Aboul-Ella, F. 1978*b*. Stiffness and damping of piles in layered media. *In* Proceedings of Earthquake Engineering and Soil Dynamics, ASCE Specialty Conference, Pasadena, Calif., 19-21 June 1978. ASCE, New York. pp. 704–719.

Novak, M., and El Sharnouby, B. 1983. Stiffness constants of single piles. Journal of Geotechnical Engineering, **109**(7): 961–974. doi:10.1061/(ASCE)0733-9410(1983)109:7(961).

Novak, M., and Grigg, R.F. 1976. Dynamic experiments with small pile foundations. Canadian Geotechnical Journal, **13**(4): 372–385. doi:10.1139/t76-039.

Novak, M., and Sheta, M. 1980. Approximate approach to contact problems of piles. *In* Proceedings of Specialty Session, ASCE National Convention on Dynamics Response of Pile Foundations: Analytical Aspects, 30 October 1980. ASCE, New York. pp. 53–79.

Novak, M., Nogami, T., and Aboul-Ella, F. 1978. Dynamic soil reactions for plane strain case. Journal of the Engineering Mechanics Division, ASCE, **104**(EM4): 953–959.

O'Neill, M.W. 2001. Side resistance in piles and drilled shafts. Journal of Geotechnical and Geoenvironmental Engineering, **127**(1): 3–16. doi:10.1061/(ASCE)1090-0241(2001)127:1(3).

Penzien, J. 1970. Soil-pile foundation interaction. *In* Earthquake engineering. Prentice-Hall, Inc., New Jersey.

Randolph, M.F., Carter, J.P., and Wroth, C.P. 1979. Driven piles in clay-the effects of installation and subsequent consolidation. Géotechnique, **29**(4): 361–393. doi:10.1680/geot.1979.29.4.361.

Sakr, M. 2009. Performance of helical piles in oil sand. Canadian Geotechnical Journal, **46**(9): 1046–1061. doi:10.1139/T09-044.

Sheta, M., and Novak, M. 1982. Vertical vibration of pile groups. Journal of the Geotechnical Engineering Division, ASCE, **108**(4): 570–590.

Sy, A., and Siu, D. 1992. Forced vibration testing of an expanded base concrete pile. *In* Proceedings of Specialty Session, ASCE National Convention on Piles under Dynamic Loads, 13-17 September 1992., Geotechnical Special Publication No. 34. ASCE, New York. pp. 170–186.

Veletsos, A.S., and Verbič, B. 1973. Vibration of viscoelastic foundations. Earthquake Engineering and Structural Dynamics, **2**(1): 87–102. doi:10.1002/eqe.4290020108.

Wolf, J.P., Meek, J.W., and Song, C. 1992. Cone models for a pile foundation. *In* Proceedings of Specialty Session, ASCE National Convention on Piles under Dynamic Loads, 13-17 September 1992. Geotechnical Special Publication No. 34. ASCE, New York. pp. 94–113.

Zhang, D.J.Y. 1999. Predicting capacity of helical screw piles in Alberta soils. M.E.Sc. thesis, University of Alberta, Edmonton, Alta.